IMA Journal of Management Mathematics (2004) **15**, 321–337

Optimization techniques for Available Transfer Capability (ATC) and market calculations

SUNG-KWAN JOO AND CHEN-CHING LIU
Department of Electrical Engineering, University of Washington, Seattle WA 98195, USA

YANGFANG SHEN AND ZELDA B. ZABINSKY
Department of Industrial Engineering, University of Washington, Seattle WA 98195, USA

AND

JACQUES LAWARREE
Department of Economics, University of Washington, Seattle WA 98195, USA

The recent movement towards an open, competitive market environment introduced new optimization problems such as market clearing mechanism, bidding decision and Available Transfer Capability (ATC) calculation. These optimization problems are characterized by the complexity of power systems and the uncertainties in the electricity market. Accurate evaluation of the transfer capability of a transmission system is required to maximize the utilization of the existing transmission systems in a competitive market environment. The transfer capability of the transmission networks can be limited by various system constraints such as thermal, voltage and stability limits. The ability to incorporate such limits into the optimization problem is a challenge in the ATC calculation from an engineering point of view. In the competitive market environment, a power supplier needs to find an optimal strategy that maximizes its own profits under various uncertainties such as electricity prices and load. On the other hand, an efficient market clearing mechanism is needed to increase the social welfare, i.e. the sum of the consumers' and producers' surplus. The need to maximize the social welfare subject to system operational constraints is also a major challenge from a societal point of view. This paper presents new optimization techniques motivated by the competitive electricity market environment. Numerical simulation results are presented to demonstrate the performance of the proposed optimization techniques.

Keywords: Markov decision process; market optimization; improving hit-and-run; power system economics; available transfer capability.

1. Introduction

Optimization techniques have been applied to various traditional power system problems including minimization of generation costs and system losses. Various optimization tools have been developed to solve optimal power flow, economic dispatch and unit commitment (Wood & Wollenberg, 1996). These problems are complex due to both the nonlinear nature of power flows and a large number of continuous or discrete decision variables and constraints. The recent movement towards an open, competitive market environment introduced new optimization problems such as market clearing mechanism, bidding decision and available transfer capability (ATC) calculation. These new optimization problems become more complicated due to the complexity of power systems and the uncertainties in the electricity market.

In a competitive market environment, the system operator needs to know how much additional power can be transferred from one area to another area without violating system constraints. Accurate evaluation of the transfer capability of a transmission system is required to maximize the utilization of the existing transmission systems. In practice, the transfer capability of the transmission networks can be limited by various system constraints such as thermal, voltage and stability limits (Gravener *et al.*, 1999). The ability to incorporate such limits into the optimization problem is a challenge in the ATC calculation from an engineering perspective.

In a deregulated power market where electric power is traded through spot and bilateral markets, a power supplier chooses an optimal strategy to maximize its own profits under various uncertainties such as electricity prices and load. Rotting & Gjelsvik (1993) and Kaye *et al.* (1990) proposed optimization-based methods for scheduling of bilateral contracts. Song *et al.* (2000) used a Markov decision process (MDP) model to find an optimal bidding strategy in the spot market environment. In trading, a power supplier needs to find optimal coordination of the bilateral contracts and spot market bidding decision while taking into account the supplier's production limit. Therefore, maximization of the combined profits in both markets requires optimization of the combined problem rather than optimization of each individual problem. On the other hand, from a societal point of view, an efficient market clearing mechanism is needed to increase the social welfare that is the sum of the consumers' and producers' surplus. The need to maximize the social welfare subject to system operational constraints is also a major challenge from a societal point of view.

This paper presents state-of-the-art optimization techniques: (i) to maximize the power transfer between areas, (ii) to maximize the expected profit for a power supplier, and (iii) to maximize social welfare in a competitive market environment. The sensitivity of the energy margin can provide information on how changes in generations can influence the degree of stability of a system (Fouad & Vittal, 1992). The proposed ATC method determines ATC between areas by running a series of numerical simulations directed by energy margin sensitivity as well as energy margin. The decision-making process of the bilateral contract affects the bidding strategy to the spot market since bidding decision-making in electricity markets is coupled with the bilateral contract position. An MDP-based optimization technique is intended to assist a market participant to make decisions on bilateral contracts and bidding to the spot market. Given the nonlinearity of power systems, the market optimization problem (MOP) requires the use of the global optimization technique to maximize the social welfare of a market. A global optimization algorithm in combination with sequential quadratic programming (SQP) is applied to solve the MOP incorporating the complex characteristics of large-scale nonlinear power systems.

The remainder of this paper is organized as follows. In Section 2, the ATC calculation problem, suppliers' optimization problem (SOP) and MOP are formulated with the power system model incorporating the nonlinear nature of power systems. Section 3 presents optimization techniques to solve the problems described in Section 2.

2. Problem description

2.1 *Available Transfer Capability*

According to the report of NERC (1995), transfer capability refers to the ability of transmission systems to reliably transfer power from one area to another over all transmission paths between those areas under given system conditions. The mathematical definition of ATC given in the report of NERC (1996) is ‘ … *the Total Transfer Capability (TTC) less the Transmission Reliability Margin (TRM), less the sum of existing transmission commitments and the Capacity Benefit Margin (CBM)*’:

$$\text{ATC} = \text{TTC} - \text{TRM} - \text{existing transmission commitments (including CBM).} \tag{2.1}$$

TTC refers to the maximum amount of electric power that can be transferred over transmission systems without violating system security constraints. The accuracy of the ATC calculation is highly dependent on the accuracy of available network data, load forecast, and the estimation of future energy transactions. Therefore, there is uncertainty in ATC calculation associated with errors in load forecast and estimation of future energy transactions. TRM is a safety margin to protect against the overload of the transmission system considering those uncertain factors in ATC calculation. ‘Existing transmission commitments’ means ‘existing transfers between areas’. The ATC between two areas provides an indication of the maximum amount of additional MW transfer possible between two parts of a power system.

ATC between areas can be calculated by increasing generation in the sending area and at the same time increasing the same amount of load in the receiving area until the power system reaches system limits. The evaluation of ATC can be formulated as an optimization problem. The objective function to be maximized is expressed as

$$\max \sum_{i \in \text{area A}} \Delta P_i \tag{2.2}$$

subject to

$$\dot{x} = f(x, y) \tag{2.3}$$

$$0 = g(x, y) \tag{2.4}$$

$$0 \leqslant P_i + \Delta P_i \leqslant P_i^{\max} \tag{2.5}$$

$$-F^{\max} \leqslant F(x, y) \leqslant F^{\max} \tag{2.6}$$

$$V^{\min} \leqslant V \leqslant V^{\max} \tag{2.7}$$

$$EM(x, y) > 0, \tag{2.8}$$

where P_i is power injection at the bus of generator ‘i’ and $\sum_{i \in \text{area A}} \Delta P_i$ is the sum of the increased generation in the sending area A, x is a vector of state variables and y is a vector of algebraic variables. Equation (2.3) represents differential equations describing the dynamic behaviours of the power system while (2.4) represents algebraic equations including power flow equations. Equations (2.5)–(2.8) are inequality constraints. $P_i^{\max}$ is the upper limit of active power output of generator ‘i’. $F^{\max}$ is the vector of thermal limits of transmission lines. $V^{\min}$ and $V^{\max}$ are the vectors of lower and upper limits of bus voltage magnitudes, respectively. $EM(x, y)$ is energy margin which provides a quantitative measure of the degree of stability of power systems (Fouad & Vittal, 1992). The energy margin of a power system indicates how far the power system is from the stability boundary. The technical details for computing the second-kick-based energy margin of the system can be found in the work of Hashimoto *et al.* (2002).

The limiting conditions of transmission systems can shift among thermal, voltage, and stability limits as the operating condition of the power system change over time. Stability limits of systems may become more restrictive than static limits depending on system operating conditions. The ATC calculation must be evaluated based on the most restrictive one of those limiting factors. Therefore, the accuracy of ATC calculation is not reliable if the stability limits of the system are not taken into account. It is desirable to consider stability limits in addition to static limits in the ATC calculation.

2.2 *Suppliers' optimization problem*

In a competitive market environment, power suppliers choose their optimal strategies to maximize their own profits. A power supplier may participate in a bilateral market in addition to a spot market. A supplier's existing bilateral contracts would influence its bidding decision to the spot market since the total amount of electricity that can be simultaneously traded in both markets is restricted by its capacity limit. Therefore, a supplier's scheduling of bilateral contract needs to be coordinated with its bidding decisions to spot market in order to maximize the combined profits (Joo & Liu, 2000).

This study assumes that a power supplier has an obligation to provide a certain contract volume over a time horizon. The power supplier with bilateral obligations decides the scheduling of the bilateral contracts and simultaneously chooses a bidding strategy to the spot market to maximize the total profit over the planning horizon. In this section, an MDP-based optimization technique is used to find a supplier's optimal decisions over the planning horizon. A MDP consists of four elements such as states, decision options, transition probabilities, and rewards (Howard, 1960). The MDP provides a multi-stage decision model where the status of a system is represented by a stochastic process with decision options that induce stochastic transitions from one state to another state.

Power suppliers submit bids to the spot market to sell electricity. The spot prices are determined by the bids from power suppliers and the load demand. Hence, the bidding behaviours of market players will be affected by the spot price, the load demand and tomorrow's load forecast. Scheduling of the flexible bilateral contract is considered as the decision-making process that affects bidding strategy to the spot market. With this in mind, the state of electricity markets is defined by all possible combinations of RCV (remaining contract volume) of a given bilateral contract, spot price, cleared-demand and tomorrow's load forecast in the spot market. Then, the number of possible states is (the number of possible RCV) $\times$ (the number of possible spot price) $\times$ (the number of possible demand) $\times$ (the number of possible forecast_load). The number of states does not increase as the number of players or the duration of the planning horizon increases. The decision options of the power supplier consist of all possible combinations of the usage of a given flexible bilateral contract and the bidding decision to the spot market.

Transition probabilities can be modelled by statistical analysis based on competitors' bidding data, historical prices and load information. In this paper, $\Pr(t, i, k, j)$ represents the transition probability from state i to state j if the decision maker makes decision option 'k' for each time period t. The calculation of transition probability requires the identification of market scenarios, which include the other player's probabilistic bidding information as well as the decision option of the power producer. If all possible aggregate bidding data with forecasted demand in state i are put into the market clearing system, a transition can be found according to the market clearing price and RCV. Then, one must find all scenarios which contribute to state j, and add up all the probabilities of the various scenarios. The overall probability represents the transition probability from state i to state j. The availability of the competitors' bidding data is critical for the accuracy of the transition probabilities.

The power supplier earns r_{ij} dollars when the electric market system moves from state i to state j. The r_{ij} associated with the transition from state i to j is called the 'reward'. Reward is the difference between the revenue and the cost of the power supplier. For each time period t, the immediate reward of a power supplier from state i to state j with decision option 'k' is calculated as follows:

$$r(t, i, k, j) = SP(t, j) \times Q(t, j) + BCP \times x(t, k) - \text{Cost}[Q(t, j) + x(t, k)] \quad (2.9)$$

where $SP(t, j)$ = spot market price in state j at time period t, $Q(t, j)$ = power producer's quantity that is accepted into spot market in state j at time period t, $x(t, k)$ = scheduling decision of bilateral contract with decision option k at time period t, and BCP = bilateral contract price per MW. After the transition probabilities and rewards are calculated, the next step is to find the optimal decision option in the ith state that maximizes the expected value of accumulated rewards over the planning horizon. A value iteration algorithm is used to find an optimal decision option to maximize the following value iteration equation:

$$V(i, \tau + 1) = \max_{k=1}^{K} \sum_{j=1}^{N} \{\Pr(i, k, j) * [r(i, k, j) + V(j, \tau)]\} \quad (2.10)$$

where $V(i, \tau + 1)$ is the total expected reward in $\tau + 1$ remaining stages starting from state i if an optimal policy is followed. Once V is computed over the decision options, the optimal policy is immediately obtained by choosing any decision which satisfies the maximum function of the value iteration equation.

2.3 *Market Optimization Problem*

From a market point of view, it is desirable to maximize the social welfare, which is defined by the sum of the consumers' and producers' surplus. There are transmission system constraints based on the nonlinear power flow model. Generators also have their capacity availability constraints and ramping constraints that limit the rate of power that can be increased. In the work of Shen *et al.* (2003), the market mechanism problem was first formulated based on a 30-bus power flow system. The mathematical optimization model based on a general power flow system to find the optimal combination of the power generated, $P_1, \ldots, P_m$, and the load delivered, $L_1, \ldots, L_n$, to maximize the social welfare is stated below.

$$\max \sum_{i=1}^{n} U_{L_i} - \sum_{j=1}^{m} C_{P_j} \quad (2.11)$$

where producers' cost function

$$C_{P_j} = \alpha_j P_j^2 + \beta_j P_j + \gamma_j \quad \text{for } j = 1, \ldots, m \tag{2.12}$$

and consumers' gross surplus function

$$U_{L_i} = -\upsilon_i L_i^2 + \nu_i L_i \qquad \text{for } i = 1, \ldots, n \tag{2.13}$$

subject to

$$L_i^{\min} \leqslant L_i \leqslant L_i^{\max} \qquad \text{for } i = 1, \ldots, m \tag{2.14}$$

$$P_j^{\min} \leqslant P_j \leqslant P_j^{\max} \qquad \text{for } j = 1, \ldots, n \tag{2.15}$$

$$-F_{bk}^{\max} \leqslant \frac{\sin(\theta_b - \theta_k)}{x_{b\_k}} \leqslant F_{bk}^{\max} \text{ for all connected buses } b, k, (b < k) \tag{2.16}$$

$$\sum_{\substack{k:\text{bus } k \text{ is} \\ \text{connected} \\ \text{to bus } b}} \frac{\sin(\theta_b - \theta_k)}{x_{b\_k}} = 0 + P_{g(b)} - L_{l(b)} \quad \text{for } b = 1, \ldots, B \tag{2.17}$$

where α_j, β_j and γ_j are the parameters of the generator j's cost function, ν_i, υ_i are the parameters of the load i's gross consumer surplus function, $P_j^{\max}$, $P_j^{\min}$ and $L_i^{\max}$, $L_i^{\min}$ represent the upper and lower bounds of the jth generator and the ith load respectively, $F_{bk}^{\max}$ is the capacity of the transmission line that connects bus b and bus k, and x_{b_k} is the reactance of the line. In the balance equation constraints, $g(b)$ is the generator number connected to bus b and $l(b)$ is the load number connected to the bus. Note that if there is no generator or load connected to the bus, the right-hand side of the balance equation equals zero.

Unlike the traditional optimal power flow model used by Sun *et al.* (1984) and Alsac *et al.* (2003), the power flow equations considered here in the MOP model are nonlinear functions, involving sinusoidal functions. This is more difficult for existing optimization techniques. If the objective function and intersection of nonlinear constraints are convex, then local optimization techniques may be applied, such as SQP (Boggs & Tolle, 1995). However, a complex power system may have a non-convex feasible region. Shen *et al.* (2003) showed that by using SQP with the starting point being chosen by trial and error, two different local optima were found for the MOP based on a 30-bus power flow system. The nonlinear and global nature of the problem would imply that other optimization techniques are necessary. Currently, simulated annealing and genetic algorithms are employed for complex global optimization problems in other arenas with little underlying structure (see Pham & Karaboga, 2000). In Section 3.3, Improving Hit-and-Run (Zabinsky *et al.*, 1993) will be combined with SQP to solve an example of MOP with a two-area, four-machine test system.

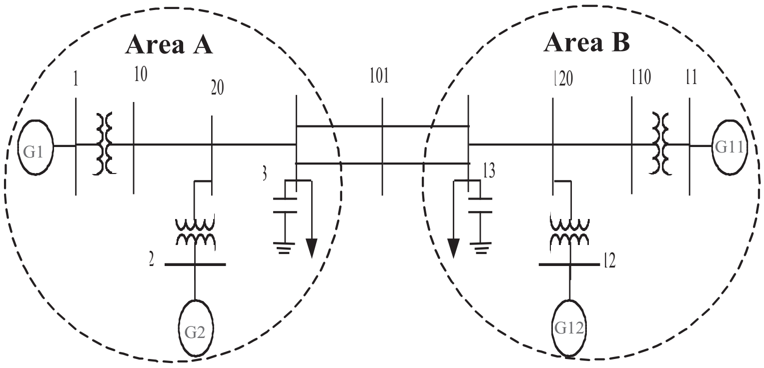

FIG. 1. Two-area four-machine test system.

3. Optimization techniques for ATC and market calculations

In this section, new optimization techniques will be illustrated with a small competitive electricity market and the two-area four-machine test system, which consists of four generators, 11 buses and 12 transmission lines as shown in Fig. 1. The generators are modelled via the sub-transient model, and are equipped with exciters, while the loads are constant MVA. The two-area four-machine test system is divided into two areas: A and B. Area A includes generators 1 and 2, which generate electricity P_1 and P_2, while area B includes generators 11 and 12, which generate electricity P_3 and P_4. The loads delivered to two customers are L_1 and L_2, which are located in area A and area B respectively. Both areas are connected to the bus 101 with two identical parallel lines.

3.1 *Optimization technique to calculate ATC*

The proposed method determines ATC between areas by running a series of numerical simulations while examining whether the system limit is reached. The proposed method to calculate ATC consists of three major procedures: (i) second-kick-based energy margin computation, (ii) energy margin sensitivity computation, and (iii) generation adjustment. The proposed ATC method first performs numerical simulations to compute the second-kick-based energy margin of the system. Once the energy margin computation is done, the energy margin sensitivity of the system is evaluated. After evaluation of energy margin sensitivity, a line search is performed along the search direction formed by the energy margin sensitivity to find the proper adjustments of generation in the sending area to increase the power transfer between areas while keeping the system below the system limit. The proposed ATC calculation algorithm can be summarized as follows.

Second-kick-based energy margin computation

Step 1: Perform time-domain simulation to obtain the system trajectory following a pre-specified disturbance sequence.

Step 2: Compute potential energy of first- and second-kick trajectories.

Step 3: Calculate the potential energy difference at the respective peaks of the first-kick and second-kick disturbances for the energy margin.

Step 4: Stop if $0 < EM < \varepsilon$. (ε represents a pre-specified tolerance value). Else go to Energy Margin Sensitivities computation procedure.

Energy margin sensitivities computation

Step 5: Perform the trajectory sensitivity analysis to obtain the trajectory sensitivity to changes in generations of generators in sending area.

Step 6: Calculate $\frac{\partial EM}{\partial P_{m,i}}$, the energy margin sensitivity with respect to change in generations of generator 'i'.

Step 7: Generate the search direction by updating an approximation to the inverse of Hessian matrix. The search direction in the 'kth' iteration with the Broyden–Fletcher–Goldfarb–Shanno (BFGS) method (see Bazaraa *et al.*, 1993 and Luenberger, 1989) is generated by

$$S^{(k)} = \begin{bmatrix} S_i^{(k)} \\ \vdots \\ S_n^{(k)} \end{bmatrix} = -D^{(k)} \begin{bmatrix} \left(\dfrac{\partial EM}{\partial P_{m,i}^{(k)}}\right) \\ \vdots \\ \left(\dfrac{\partial EM}{\partial P_{m,n}^{(k)}}\right) \end{bmatrix}. \tag{3.1}$$

$D^{(k)}$ starts with an identity matrix in the first iteration and successively approximates the inverse of the Hessian matrix throughout the iterative process. The updating formula for the BFGS method to obtain $D^{(k+1)}$ is

$$D^{(k+1)} = D^k + \left(\frac{1 + (q^k)^T D^k q^k}{(q^k)^T p^k}\right) \frac{p^k (p^k)^T}{(p^k)^T q^k} - \frac{p^k (q^k)^T D^k + D^k q^k (p^k)^T}{(q^k)^T p^k} \tag{3.2}$$

where

$$p^k = \begin{pmatrix} P_{m,i}^{(k+1)} \\ \vdots \\ P_{m,n}^{(k+1)} \end{pmatrix} - \begin{pmatrix} P_{m,i}^{(k)} \\ \vdots \\ P_{m,n}^{(k)} \end{pmatrix} \quad \text{and} \quad q^k \begin{bmatrix} \left(\dfrac{\partial EM}{\partial P_{m,i}^{(k+1)}}\right) \\ \vdots \\ \left(\dfrac{\partial EM}{\partial P_{m,n}^{(k+1)}}\right) \end{bmatrix} - \begin{bmatrix} \left(\dfrac{\partial EM}{\partial P_{m,i}^{(k)}}\right) \\ \vdots \\ \left(\dfrac{\partial EM}{\partial P_{m,n}^{(k)}}\right) \end{bmatrix}. \tag{3.3}$$

Generation adjustment

Step 8: Determine the adjustments of generations of the sending area using the following equation:

$$\begin{bmatrix} \Delta P_{m,i} \\ \vdots \\ \Delta P_{m,n} \end{bmatrix} = \begin{bmatrix} \alpha_i^{(k)} \times \left(S_i^{(k)}\right)^{-1} \\ \vdots \\ \alpha_n^{(k)} \times \left(S_n^{(k)}\right)^{-1} \end{bmatrix} \times EM = k_p \begin{bmatrix} P_{m,i} \\ \vdots \\ P_{m,n} \end{bmatrix} \tag{3.4}$$

where $\sum_{i \in \text{area A}} \alpha_i^{(k)} = 1$. $\alpha_i^{(k)}$ and k_p are introduced to distribute the energy margin to each generator such that generators in the sending area are adjusted in proportion to their generations in the basecase. If the sending area includes only one generator, the generation of the generator in the sending area is adjusted using the following equation:

$$\Delta P_{m,i} = \left(S_i^{(k)}\right)^{-1} \times EM. \tag{3.5}$$

Step 9: Update generations of the sending area using the following equation:

$$\begin{bmatrix} P_{m,1}^{new} \\ \vdots \\ P_{m,k}^{new} \end{bmatrix} = \begin{bmatrix} P_{m,1}^{old} \\ \vdots \\ P_{m,k}^{old} \end{bmatrix} + \begin{bmatrix} \Delta P_{m,1} \\ \vdots \\ \Delta P_{m,k} \end{bmatrix}. \tag{3.6}$$

Step 10: Go to second-kick-based Energy Margin Computation procedure and repeat algorithms with rescheduled generations.

The proposed ATC calculation method will be illustrated with the two-area four-machine test system. First, it is necessary to establish a basecase, in which the system load is supplied without violating any system limits such as thermal, voltage and stability limits. The power transferred from area A to area B in the established basecase is equal to 453 MW. In the following example, the proposed ATC calculation method attempts to determine ATC from area A to area B by increasing generation in area A and simultaneously increasing the same amount of load at bus 13 in area B while examining whether stability limits are reached.

EXAMPLE 1 It is assumed in this example that the generation of generator 2 in area A is adjusted to increase power transfer from area A to area B while holding the generation of generator 1 in area A. This assumption is made to calculate a point-to-point ATC from bus 2 in area A to bus 13 in area B. Energy margin computation and energy margin sensitivity analysis were performed with the established basecase. The second-kick scenario consists of a temporary three-phase fault at bus 3, followed by another temporary three-phase fault at bus 20. The duration of the second-kick, which is a three-phase fault at bus 20, is selected such as to yield a marginally stable trajectory. Results of the proposed ATC calculation method for Example 1 are summarized in Table 1.

As can be seen in Table 1, the energy margin is reduced from iteration to iteration. In the fourth iteration, the proposed ATC calculation algorithm stops since the energy margin

TABLE 1 *Results of proposed ATC calculation method for Example* 1

Iteration	Power transfer (bus 2 → bus 13) (MW)	Energy margin	$P_{m,2}$ (MW)	S_2	$\Delta P_{m,2}$ (MW)
1	453	13·35	754	1·4688	9·19
2	462	10·72	763·09	0·7853	13·65
3	475·8	2·77	776·74	1·5697	1·77
4	477·3	0·11	778·41	0·5799	0·18

is less than the pre-specified tolerance value (0·5 p.u.). The transfer amount (477·3 MW) from bus 2 to bus 13 in the fourth iteration is the total transfer capability (TTC). Once TTC is obtained, a point-to-point ATC from bus 2 to bus 13 can be calculated by using (2.1).

3.2 *Optimization technique to solve SOP*

A small competitive electric market is used to illustrate the MDP-based optimization technique for the SOP. The small competitive electric market consists of the spot market, two competing power suppliers, a group of customers, and GencoA, which is the decision-making power supplier using the proposed MDP-based optimization technique. GencoA and two competing power suppliers participate in the spot market to sell electricity. This simple market model is useful only as an illustrative example and is not fully representative of an actual market.

Suppose that GencoA has a flexible contract to provide 50 MW (@$20/MW) of power with the contract partner 'A' over the course of the next week. The power must be delivered under the restriction of 10 MW per day or 0 MW per day. Thus, the number of possible RCVs is 6, i.e. 50 MW remaining on the contract, 40 MW remaining, and so on down to 0 MW remaining. To reduce the size of the state space, the spot market is restricted to generate only 'high spot price' (=$23/MW), 'medium spot price' (=$22/MW) and 'low spot price' (=$21/MW) while the possible load range is restricted to take the form of high (=350MW), medium (=320MW) and low demand (=290MW). A further reduction in states can be achieved by the assumption that the high (medium or low) spot price is related only to the high (medium or low) demand, respectively. Since this assumption does not fully represent the reality of an actual market, all possible combinations of the two variables should be considered for a practical application. Under this assumption, the number of reduced states is $54(= 6 \times 3 \times 3)$. In addition, the number of states can be further reduced by checking infeasible RCV states for each time period. For example, at the ending day of the bilateral contract, the remaining contract volume must be zero. Thus, no other than RCV = 0 MW is a feasible state at the ending day of the bilateral contract. For an illustration of states, some of the possible combinations of state variables are as follows.

- State 1: (0 MW RCV, high spot price, high demand, high forecast_load),
- State 2: (0 MW RCV, high spot price, high demand, medium forecast_load),
- State 16: (10 MW RCV, medium spot price, medium demand, low forecast_load),
- State 46: (50 MW RCV, high spot price, high demand, high forecast_load),
- State 51: (50 MW RCV, medium spot price, medium demand, low forecast_load).
- State 54: (50 MW RCV, low spot price, low demand, low forecast_load).

TABLE 2 *Decision options of GenCoA*

Option k	Description of decision options of GenCoA
1	Low-priced bidding without usage of bilateral contract ($x_t = 0$ MW)
2	Medium-priced bidding without usage of bilateral contract ($x_t = 0$ MW)
3	High-priced bidding without usage of bilateral contract ($x_t = 0$ MW)
4	Low-priced bidding with usage of bilateral contract ($x_t = 10$ MW)
5	Medium-priced bidding with usage of bilateral contract ($x_t = 10$ MW)
6	High-priced bidding with usage of bilateral contract ($x_t = 10$ MW)

State transition occurs as a result of a change in load demand and price. The MDP generates a sequence of rewards as it makes transitions from state to state over the planning horizon. The decision options of GenCoA also affect reward and transition probabilities. It is assumed that GenCoA calculate transition probabilities based on load forecast, decisions for each state, and probabilistic bidding information of two competitors. For practical applications, probabilistic bidding information of competitors needs to be modelled with statistical market data analysis. The decision option of GenCoA consists of all possible combinations of the usage of a given flexible bilateral contract and the bidding decision to the spot market. GencoA is restricted to take the form of high-priced, medium-priced or low-priced bidding to the spot market. The possible decision options of GenCoA are listed in Table 2.

Block bidding over different MW ranges is employed for GenCoA's bidding curve representation. For example, the low-priced bidding option of GenCoA without bilateral contract usage (decision option 1) will be

$$\begin{bmatrix} \text{17\$/MW over the first 50 MW} \\ \text{18\$/MW over the next 40 MW} \\ \text{19\$/MW over the next 30 MW} \\ \text{19\$/MW over the next 30 MW}\cdot \end{bmatrix}$$

If the bilateral contract usage is exercised, the bidding curve is shifted to the left in the amount of the bilateral contract usage. When GenCoA exercises the usage of the bilateral contract (10 MW) with the low-priced bidding option, the supply bidding option (decision option 4) will result in the following format:

$$\begin{bmatrix} \text{17\$/MW over the first 40 MW} \\ \text{18\$/MW over the next 40 MW} \\ \text{19\$/MW over the next 30 MW} \\ \text{19\$/MW over the next 30 MW}\cdot \end{bmatrix}$$

On the first day (or time period '$t = 1$') of the bilateral contract, GencoA makes a decision considering the entire week ahead. The value iteration algorithm is applied to find an optimal decision option to maximize the expected value of accumulated rewards over the planning horizon. Due to space limitation, selected results of the MDP-based optimization technique are shown in Table 3. According to the simulation results, the optimal decision option differs in the time period '$t = 1$' depending on the current state of the system. If the system is in state '49' which corresponds to (RCV = 50 MW, medium spot price, medium

TABLE 3 *Selected simulated results* ($t = 1$)

Feasible state i	Optimal decision option #	Contract usage (MW)	Bidding to spot market	Accumulated reward
State 46	4	10	Low-priced bidding	96768·13
State 47	6	10	High-priced bidding	123240·77
State 48	5	10	Medium-priced bidding	79920·83
State 49	4	10	Low-priced bidding	124416·17
State 50	6	10	High-priced bidding	95853·93
State 51	5	10	Medium-priced bidding	102755·35
State 52	4	10	Low-priced bidding	124416·17
State 53	6	10	High-priced bidding	95853·93
State 54	5	10	Medium-priced bidding	102755·35

demand, forecasted high demand), the optimal decision of the power producer at time period $t = 1$ is '4' which means 'low-priced bidding to the spot market with usage of the bilateral contract'. In last time period '$t = 7$', GenCoA's optimal decision is the decision option that gives maximum daily reward because GenCoA does not need to consider the effect of bidding strategy beyond the planning horizon.

3.3 *Optimization technique to solve MOP*

In this section, our focus is on solving the MOP based on the two-area test system. The parameters of the model are given in the Appendix. Considering the sinusoidal function involved in the power flow constraints that may cause a non-convex feasible region we will use a global optimization algorithm combining with SQP to solve the model. Particularly, we will implement Improving Hit-and-Run (IHR) to solve the model directly, then provide the solution found by IHR as the starting point of SQP and use SQP to find the local optimum. A multi-start approach will be used to improve the probability of finding a global optimum.

IHR was introduced by Zabinsky *et al.* (1993) as a sequential random search global algorithm in a measurable continuous domain. The main idea behind IHR is to use a line sampler called Hit-and-Run, which was introduced by Smith (1984) as a Markov chain Monte Carlo sampler, to generate candidate points, then select those that are improving in objective function value. It was shown that IHR converges to a global optimum with probability one for a broad class of global optimization problem. In addition, the expected number of function evaluations of IHR on the class of positive definite quadratic programs is polynomial in the dimension n, and specifically, $O(n^{5/2})$ (Zabinsky *et al.*, 1993). IHR can be formally described as follows.

Improving Hit-and-Run algorithm

Step 0: Initialize starting point X_0 randomly in the feasible region S, and set $k = 0$.

Step 1: Generate a random direction D_k according to a uniform distribution on a unit n-dimensional hyper-sphere.

Step 2: Generate a point Y_{k+1} uniformly distributed on the line set

$$L = S \cap \{x | x = X_k + \lambda D_k, \lambda \text{ a real scalar}\}. \tag{3.7}$$

Step 3: If the objective function value at the point Y_{k+1} is better than that at the point X_k, set $X_{k+1} = Y_{k+1}$. Otherwise, set $X_{k+1} = X_k$.

Step 4: If a stopping criterion is satisfied, then stop. Otherwise increment k and return to step 1.

In contrast to IHR, the SQP method is a deterministic algorithm that searches for a local optimum nearest to a given starting point. At each iteration of SQP, an approximation is made of the Hessian of the Lagrangian function. This is then used to generate a quadratic programming sub-problem involving the minimization of a quadratic approximation of the objective function, subject to a linear approximation of the constraints. The solution of the sub-problem is then used to form a search direction for a line search procedure. An overview of SQP is found in Boggs & Tolle (1995).

As a deterministic algorithm, SQP is not a suitable algorithm for a global optimization problem. The performance of SQP is very sensitive to the initial starting point, which influences which local optimum is detected. Therefore, instead of using SQP to solve the MOP directly, it is proposed to first use IHR, the global optimization algorithm, to find a good starting point, and then use SQP to search for the local optimum nearest to the starting point. In order to improve the probability of finding the global optimum, a multi-start approach with our mixed algorithm will be used to solve the model. Particularly, in our code, the mixed algorithm will be run 50 times, and for each run, the maximum number of iterations of IHR is 100 and the maximum number of iterations of SQP is 500.

A difficult step in the two-area MOP is to solve for bus angles embedded within the optimization algorithm. Instead of choosing $P_1, \ldots, P_4$ and L_1, L_2 as decision variables, our approach is to choose angle differences as decision variables. Particularly, five angle differences, $(\theta_1 - \theta_{10})$, $(\theta_2 - \theta_{20})$, $(\theta_3 - \theta_{101})$, $(\theta_{13} - \theta_{120})$ and $(\theta_{12} - \theta_{120})$, are chosen as decision variables, and the values of other angle differences and $P_1, \ldots, P_4, L_1, L_2$ are the functions of the five decision variables. Considering the nature of the sinusoidal function, it is reasonable to set the upper and lower bounds of each decision variable to be $-90°$ and $90°$.

In our mixed algorithm, IHR is used to obtain a good starting point for SQP. Considering the difficulties for IHR to handle inequality and equality constraints, those constraints are put into the objective function by adding a penalty on violated constraints. Therefore the feasible region S for IHR becomes a five-dimensional box with $-90°$ and $90°$ as the upper and lower bounds of angle difference, i.e.

$$S = \left\{(\Delta\theta_1, \ldots, \Delta\theta_5) : \Delta\theta_i \in \lfloor -90°, 90° \rfloor, \text{ for } i = 1, \ldots, 5\right\}. \tag{3.8}$$

It may cause the problem that, under some combination of decision variables in S, there may exist complex numbers for other angle differences in the model. This drawback is also considered in the objection function by adding another penalty. The penalty objective function used for IHR is therefore as follows:

$$\max \qquad f(\Delta\theta) = \sum_{i=1}^{4} U_{L_i} - \sum_{j=1}^{2} C_{P_j} - \mu \tag{3.9}$$

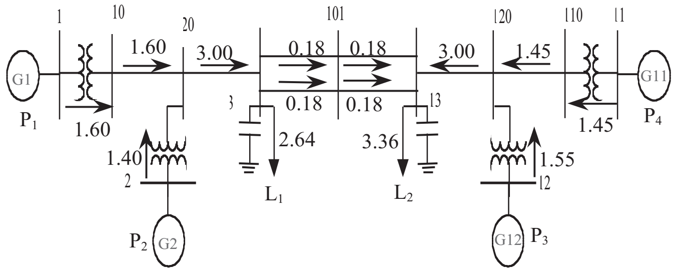

FIG. 2. Optimal solution of two-area MOP.

where

$$C_{P_j} = \alpha_j P_j^2 + \beta_j P_j + \gamma_j \quad \text{for } j = 1, \dots, 4 \tag{3.10}$$

$$U_{L_i} = -\nu_i L_i^2 + \nu_i L_i \quad \text{for } i = 1, 2 \tag{3.11}$$

$$\mu = \begin{cases} 10^8 & \text{if complex number exists in the model} \\ \kappa \cdot 10^6 & \text{otherwise} \end{cases} \tag{3.12}$$

where κ is the total number of violated constraints in the original MOP model. The result of an IHR run on the penalty function problem is then taken as a starting point for SQP on the original MOP formulation. The mixed algorithm is run 50 times with the starting point of IHR being chosen uniformly over the set S. Among the 50 runs, the mixed algorithm successfully found an optimal solution 37 times, and failed to find an optimal solution 13 times. Of the unsuccessful runs, four runs ended by exceeding the maximum number of iterations of SQP, and nine runs ended SQP with an infeasible solution. An interesting observation on the successful runs is that they all converge to the same local optimum, which is shown in Fig. 2 and Table 4. This may be because of the relatively simple structure of the two-area power flow system. While it is difficult to prove mathematically that the solution found by the mixed algorithm is a global optimum, by using the mixed algorithm with a multi-start approach, we can announce with confidence that we have found a global optimum.

In order to explore the benefit of using IHR, the SQP itself is also run 50 times with starting points generated uniformly over the set S. Among 50 runs, eight runs found the same optimal solution successfully; 24 runs ended at an infeasible solution and 18 runs ended by exceeding the maximum number of iterations of SQP. Hence coupling IHR with SQP provides a more robust mixed algorithm.

4. Conclusions

In this paper, new optimization techniques are proposed to deal with ATC calculation, SOP, and MOP which are motivated by the competitive electricity market environment. The proposed ATC calculation method is designed to incorporate system dynamics in the ATC calculation and to avoid exhaustive numerical simulations directed by energy margin and energy margin sensitivity. The BFGS method was employed to speed up the convergence of the ATC calculation process. An MDP-based optimization technique is proposed for optimal coordination of the bilateral contracts and spot market bidding decisions. A

TABLE 4 *Optimal solution of two-area MOP*

Decision variables: $\theta_1 - \theta_{10} = 1{\cdot}5311°$, $\theta_2 - \theta_{20} = 1{\cdot}3397°$, $\theta_3 - \theta_{101} = 1{\cdot}1380°$, $\theta_{13} - \theta_{120} = -1{\cdot}7191°$, $\theta_{12} - \theta_{120} = 1{\cdot}4858°$			
	Bus angle (set $\theta_1 = 0°$)		Bus angle (set $\theta_1 = 0°$)
Bus 1	$0°$	Bus 11	$-2{\cdot}6409°$
Bus 10	$-1{\cdot}5311°$	Bus 110	$-4{\cdot}0260°$
Bus 20	$-3{\cdot}8236°$	Bus 120	$-6{\cdot}0996°$
Bus 2	$-2{\cdot}4839°$	Bus 12	$-4{\cdot}6138°$
Bus 3	$-5{\cdot}5427°$	Bus 13	$-7{\cdot}8188°$
Bus 101	$-6{\cdot}6807°$		
Maximum social welfare = 13893			

global optimization algorithm, IHR, combined with the traditional SQP is introduced to solve marketing optimization problems. The proposed optimization techniques were implemented and tested on the two-area four-machine test system. The test results have shown the effectiveness of the proposed optimization techniques.

Many other opportunities exist for the application of optimization techniques to electricity market problems. Uncertainties in the market price require statistical forecasting techniques. Prediction of the market behaviour is a natural problem for heuristic computational methods. The concept of efficient frontier in finance for risk management requires multi-objective optimization and the concept of Pareto optimality. Market clearing mechanisms may involve combinatorial optimization to select generating units to meet the load demand. The determination of a market equilibrium given a number of supply and demand bids is an optimization problem.

Acknowledgements

This research is partially supported by the Advanced Power Technologies (APT) Centre at the University of Washington and the U.S. National Science Foundation Under Grant 'Transmission Expansion in an Open Access Environment: Reliability and Economics (ECS 0217701)'. The APT Centre is funded by AREVA T&D, BPA, CESI, LGIS, Mitsubishi Electric, PJM and RTE.

REFERENCES

ALSAC, O., BRIGHT, J., PRAIS, M. & STOTT, B. (1990) Further developments in lp-based optimal power flow. *IEEE Trans. Power Syst.*, **5**, 697–711.

BAZARAA, M. S., SHERALI, H. D. & SHETTY, C. M. (1993) *Nonlinear Programming*. New York: Wiley, pp. 325–327.

BOGGS, P. T. & TOLLE, J. W. (1995) Sequential quadratic programming. *Acta Numer.*, **4**, 1–51.

FOUAD, A. A. & VITTAL, V. (1992) *Power System Transient Stability Analysis Using the Transient Energy Function Method*. Englewood Cliffs, NJ: Prentice-Hall.

GRAVENER, M. H., NWANKPA, C. & YEOH, T. (1999) ATC computational issues. *Proc. 32nd Hawaii Int. Conf. on System Sciences*. pp. 1–6.

HOWARD, R. A. (1960) *Dynamic Programming and Markov Process*. New York: MIT Press.

JOO, S. K. & LIU, C. C. (2000) Electricity market simulation based on a markov decision model. *Proc. 4th Int. Conf. on Power Systems Operation and Planning*. pp. 102–103.

KAYE, R.J., OUTHRED, H. R. & BANNISTER, C. H. (1990) Forward contracts for the operation of an electricity industry under spot pricing. *IEEE Trans. Power Syst.*, **5**, 46–52.

LUENBERGER, D. G. &, (1989) *Linear and Nonlinear Programming*. Reading, MA: Addison-Wesley, pp. 268–271.

NORTH AMERICAN ELECTRIC RELIABILITY COUNCIL (1995) *Transmission Transfer Capability*. Princeton, NJ: NERC.

NORTH AMERICAN ELECTRIC RELIABILITY COUNCIL (1996) *Available Transfer Capability Definitions and Determination*. Princeton, NJ: NERC.

PHAM, D. T. & KARABOGA, D. (2000) *Intelligent Optimisation Techniques: Genetic Algorithms, Tabu Search, Simulated Annealing and Neural Networks*. London: Springer.

ROTTING, T. A. & GJELSVIK, A. (1993) Stochastic dual dynamic programming for seasonal scheduling in the Norwegian power system. *IEEE Trans. Power Syst.*, **7**, 273–279.

SHEN, Y., LAWARRÉE, J., LIU, C. C. & ZABINSKY, Z. B. (2003) Global optimization in an electricity market environment. *Proc. IEEE Bologna Power Tech*.

SMITH, R. L. (1984) Efficient Monte Carlo procedures for generating points uniformly distributed over bounded region. *Oper. Res.*, **32**, 1296–1308.

SONG, H., LIU, C. C., LAWARRÉE, J. & DAHLGREN, R. (2000) Optimal electricity supply bidding by Markov decision process. *IEEE Trans. Power Syst.*, **15**, 618–624.

SUN, D., ASHLEY, B., BREWER, B., HUGHES, A. & TINNEY, W. F. (1984) Optimal power flow by Newton approach. *IEEE Trans. Power Apparatus Syst.*, **103**, 2864–2880.

WOOD, A. & WOLLENBERG, B. (1996) *Power Generation Operation and Control*. New York: Wiley.

ZABINSKY, Z. B., SMITH, R. L., MCDONALD, J. F., ROMEIJN, H. E. & KAUFMAN, D. E. (1993) Improving hit-and-run for global optimization. *J. Global Optim.*, **3**, 171–192.

Appendix

TABLE A1 *Parameters of cost functions of generators and the upper and lower bounds of generators*

Generator (P)	Lower bounds	Upper bounds	Cost function parameters		
			α	β	γ
1	0	5	100	700	300
2	0	4	150	600	100
3	0	3	200	400	150
4	0	3·5	180	500	150

TABLE A2 *Parameters of utility functions of loads*

Loads (L)	Utility function parameters ν	v
1	160	3500
2	200	4000

TABLE A3 *Capacities and reactance of transmission lines*

Connected buses Bus b	Bus k	Capacity (CAP_{bk})	Reactance (x_{b_k})
1	10	3·0	0·0167
10	20	3·0	0·0250
2	20	3·0	0·0167
20	3	3·0	0·0100
3	101 (1)	3·0	0·1100
3	101 (2)	3·0	0·1100
13	101 (1)	3·0	0·1100
13	101 (2)	3·0	0·1100
120	13	3·0	0·0100
12	120	3·0	0·0167
110	120	3·0	0·0250
11	110	3·0	0·0167

Note: $x_{b\_k} = x_{k\_b}$